Electronic Supplementary Material (ESI) for Dalton Transactions.
This journal is © The Royal Society of Chemistry 2015

Supporting Information

For

A hypoxia efficient imidazole based Ru(II) arene anticancer agent resistant to deactivation by glutathione

Kallol Purkait,‡ Subhendu Karmakar,‡ Sudipta Bhattacharyya, Saptarshi Chatterjee, Suman Kr Dey, Arindam Mukherjee*

Department of Chemical Sciences, Indian Institute of Science Education and Research Kolkata, Mohanpur campus, Mohanpur-741246, India. Fax: +91 33 2587 3020; *E-mail:* a.mukherjee@iiserkol.ac.in

‡ both the authors contributed equally

Contents

EXPERIMENTAL SECTION

Materials and methods

The chemicals and solvents used were purchased from commercial sources. The solvents used for synthetic purposes were distilled and dried prior to use[1]. Ethidium bromide (EtBr), agarose (molecular biology grade) were purchased from SRL (India). MTT [(3-(4, 5-dimethylthiazol-2-yl)-2, 5-diphenyltetrazolium bromide)] (USB) and other cell growth media and their supplements were purchased from Gibco. Imidazole-2-carboxaldehyde, 2,6-diisopropylaniline, Reduced L-Glutathione (GSH) were purchased from Sigma-Aldrich and used without any further purification. Ruthenium(III) trichloride was purchased from precious metals online, Australia. $[Ru^{II}_2(p\text{-cymene})_2Cl_4]$ was synthesized according to a literature procedure.[2] The solvents used in spectroscopy and lipophilicity measurements were of spectroscopy grade, purchased from Merck and used without any further purification. Melting points and decomposition temperatures of the compounds were measured in triplicate with one end sealed capillaries using SECOR India melting point apparatus and the uncorrected values are reported. UV-visible measurements were done using Perkin Elmer lambda 35 spectrophotometer. FT-IR spectra were recorded using Perkin-Elmer SPECTRUM RX I spectrometer in KBr pellets. ^{1}H & proton decoupled ^{13}C NMR spectra were measured using either JEOL ECS 400 MHz or Bruker Advance III 500 MHz spectrometer at 25°C. The chemical shifts are reported in parts per million (ppm). Elemental analyses were performed on a Perkin-Elmer 2400 series II CHNS/O analyzer. Electro-spray ionization mass spectra were recorded using a Q-Tof micro™ (Waters) mass spectrometer by +ve mode electrospray ionization. The recrystallization yields of isolated products are reported. The ligands and complex synthesized were dried in vacuum and stored in desiccators under dark.

Syntheses

N-((1H-imidazol-2-yl)methylene)-2,6-diisopropylaniline (L). Compound L was synthesized by modification of a reported literature procedure.[3] Imidazole-2-carboxaldehyde (0.096 g, 1 mmol) and 2,6-diisopropylaniline (0.189 ml, 1 mmol) were refluxed in ethanol in presence of catalytic amount of formic acid for 12 hours. On completion the solvent was evaporated under reduced pressure and the residue was washed with petroleum benzene. The product was further purified by recrystallization from dichloromethane. Yield: 0.190 g (75%), Anal. Calc. for $C_{16}H_{21}N_3$: C, 75.26; H, 8.29; N, 16.46; Found: C, 75.18; H, 8.34; N, 16.37%, Mp: 195°C, ^{1}H NMR (400 MHz, $CDCl_3$, 25°C): δ 8.17 (s, 1H, CH=N), 7.17 (m, 5H, Ar-H, Imi-H), 2.97 (m, 2H, CH), 1.16 (d, 12H, J = 8.6 Hz, CH_3); ^{13}C NMR: (100MHz, $CDCl_3$, 25°C): δ 153.56 (CH=N) , 146.60 (Imi-C), 144.15 (Imi-CH), 138.25 (Ar-CH), 125.56 (Ar-CH), 123.45 (Ar-C-N), 122.72 (Ar-C), 27.94 (CH-*i*Pr), 23.45(CH_3-*i*Pr). (ESI-HRMS (Methanol) m/z (calc.): 256.19 (256.19) $[C_{16}H_{22}N_3]^+$, FT-IR (KBr pellets, cm^{-1}): 2962, 1637, 1437, UV-Vis: [CH_3CN, λ_{max},nm(ε/$dm^3mol^{-1}cm^{-1}$)]: 282 (2191), 327 (308).

[(L)Ru^{II}(η^6-*p*-cym)(Cl)](PF$_6$) (1). Dichloromethane (DCM) solution of the ligand L (0.51 g, 2 mmol) was added to a DCM solution of [Ru^{II}(*p*-cym)$_2$(Cl)$_4$] (0.612 g, 1 mmol) in dark and under nitrogen atmosphere at room temperature. The solution was stirred continuously for 10 hours. After that NH_4PF_6 (0.326 g, 2 mmol) was added into the reaction mixture and stirred for another 2 hours. Evaporation of the reaction mixture led to an orange coloured mass, washed with diethyl ether. The product was purified by crystallization from a dichloromethane solution layered with petroleum benzene. Yield: 0.302 g (45%), Anal. Calc. for $C_{26}H_{35}N_3RuClPF_6$: C, 46.53; H, 5.26; N, 6.26; Found: C,46.44; H,5.19; N,6.32 %, Mp: 235°C (decomp.), ^{1}H NMR: (500MHz, DMSO-d_6, 25°C): δ 8.55 (s, 1H, CH=N), 8.22 (d, 1H, J = 1 Hz, Imi-H), 7.84 (d, 1H, J = 1 Hz, Imi-H), 7.46 (m, 2H, Ar-H), 7.36 (m, 1H, Ar-H), 5.94 (d, 1H, J = 6 Hz, *p*-cym-H), 5.51 (d, 1H, J = 6 Hz, *p*-cym-H), 5.35 (d, 1H, J = 6 Hz, *p*-cym-H), 5.25 (d, 1H, J = 6 Hz, *p*-

cym-H), 3.75 (m, 1H, CH), 2.55-2.66 (m, 2H, CH), 2.07 (s, 3H, CH_3), 1.42 (d, 3H, J = 7 Hz, CH_3), 1.23 (d, 3H, J = 6.5 Hz, CH_3), 1.10 (d, 3H, J = 7 Hz, CH_3), 1.06 (d, 3H, J = 7 Hz, CH_3), 1.03 (d, 3H, J = 7 Hz, CH_3), 0.83 (d, 3H, J = 6.5 Hz, CH_3) (Fig. S1), ^{13}C NMR: (100MHz, DMSO-d_6, 25°C): δ 159.77 (CH=N), 148.16 (Imi-C), 145.75 (Ar-C-N), 141.32 (Ar-C), 139.79 (Ar-C), 133.80 (Imi-CH), 128.57 (Ar-CH), 124.75 (Imi-CH), 124.23 (Ar-CH), 124.16 (Ar-CH), 104.80 (*p*-cym-C), 99.90 (*p*-cym-C), 85.55 (*p*-cym-CH), 84.19 (*p*-cym-CH), 83.02 (*p*-cym-CH), 82.88 (*p*-cym-CH), 30.42 (C-*i*Pr), 27.59(C-*i*Pr), 27.10 (C-*i*Pr *p*-cym), 26.57(C-*i*Pr), 25.78 (C-*i*Pr), 23.03 (CH_3-*i*Pr *p*-cym), 22.18 (CH_3-*i*Pr *p*-cym), 21.87 (CH_3-*i*Pr), 21.28 (CH_3-*i*Pr), 17.92(CH_3-*p*-cym) (Fig. S2); ESI-HRMS (Methanol) m/z (calc.): 526.16 (526.16) $[C_{26}H_{35}ClN_3Ru]^+$, FT-IR (KBr pellets,cm^{-1}): 2965, 1583, 1442, UV-Vis: [CH_3CN, λ_{max},nm (ε/$dm^3mol^{-1}cm^{-1}$)]: 305 (12864), 350 (5726).

[Ru^{II}(p-cym)(en)Cl](PF$_6$) (C1). Complex **C1** was synthesized using literature mentioned procedure[4]. Yield: 0.10 g (40%), Anal. Calc. for $C_{12}H_{22}ClF_6N_2PRu$: C, 30.29; H, 4.66; N, 5.89; Found: C,30.40; H,4.62; N,5.81 %, ^{1}H NMR: (400MHz, DMSO-d_6, 25°C): δ 6.09 (bs, 2H, NH_2), 5.58 (d, 2H, J = 5.52 Hz, *p*-cym-H), 5.41 (d, 2H, J = 5.52 Hz, *p*-cym-H), 4.16 (bs, 2H, NH_2), 2.82 (m, 1H, J = 6.4 Hz, *i*Pr-CH), 2.33 (m, 2H, CH_2), 2.19 (m, 2H, CH_2), 2.14 (s, 3H, *p*-cym-CH_3), 1.19 (d, 6H, J = 7.32 Hz, *i*Pr-CH_3) (Fig. S3).

X-ray crystallography. Good quality single crystal of **1** was obtained by layering a dichloromethane solution with petroleum ether. Single crystals of **1** was mounted using loops on the goniometer head of a Bruker Kappa Apex II CCD Duo diffractometer equipped with graphite monochromated Mo-Kα radiation (0.71073 Å) and data collected at 100 K. An empirical multi-scan absorption correction was performed using SADABS.[5] The structures were solved by direct methods and all non-hydrogen atoms were refined anisotropically by full matrix least-squares on F^2. A few important crystallographic refine parameters are summarized in Table S2. The hydrogen atoms were calculated and fixed using SHELXL-97 after

hybridization of all non hydrogen atoms.[6] The crystallographic data for the structures have been deposited at the Cambridge Crystallographic Data Centre as supplementary publication CCDC 1001374 (**1**). These data can be obtained free of charge from the Cambridge Crystallographic Data Centre via www.ccdc.cam.ac.uk/data_request/cif.

Lipophilicity. Distribution coefficient (logD) of the ligand and the complex in octanol–aqueous phosphate buffer (20 mM, pH 7.4) system was determined using standard shake-flask method.[7] Octanol and aqueous phosphate buffer (equal volume) were pre-equilibrated overnight before the experiment.[8] After equilibration the solid samples were added to the mixture of solvents and shaken on a dancing shaker for 10 hours at 37°C. After that the tubes were centrifuged and left undisturbed for an hour. Aliquots of the aqueous and octanol layers were pipetted out separately and the absorbances were measured using UV-vis spectrophotometer. Concentration of the substances in each layer was calculated using the respective molar extinction coefficients.

Cell lines and culture. Human breast adenocarcinoma (MCF-7), human lung adenocarcinoma (A549) and human cervical carcinoma (HeLa) cell lines were obtained from Department of Biological Sciences, IISER Kolkata (purchased from ATCC). Cell lines were maintained in the logarithmic phase at 37°C in 5% carbon dioxide-95% air using the cell culture media containing DMEM, 10% fetal bovine serum (GIBCO) and antibiotics (100 units ml^{-1} penicillin and 100 mg ml^{-1} streptomycin). Hypoxia cultures of MCF-7 and A549 were grown in 5% carbon dioxide and 1.5% oxygen keeping everything else the same.

Cell viability assay. The growth inhibitory studies on tumor cell lines were carried out using MTT assay. In brief, 6×10^3 cells per well, were seeded in 96-well microplates in DMEM (200 µl) followed by incubation at 37°C (5% CO_2 atmosphere). After 48 h, the DMEM was removed and replaced with fresh media containing the compounds to be studied at the appropriate concentrations. The stock solutions of compounds were prepared in DMSO such

that concentration of DMSO in well does not exceed 0.2%. Each drug concentration was added in triplicate. After completion of 48 h incubation with the compounds, the compound containing media was removed and fresh DMEM added to each well followed by treatment with 20 µl of a 1 mg ml^{-1} MTT in PBS (pH 7.2). After 3 h of incubation with MTT, media was removed and 200 µL of DMSO added to each well. The inhibition of cell growth induced by the tested complexes was detected by measuring the absorbance of each well at 515 nm using a BIOTEK ELx800 plate reader. IC_{50} value represents the drug concentration that restricts the cell survival to 50% compared to the untreated control wells.

In hypoxic condition the oxygen percentage of the CO_2 incubator (ESCO cell culture CO_2 incubator, model: CCL-170T-8-UV) was maintained at 1.5%. Compounds were loaded in 96-microwell plates in level-II biosafety cabinet under atmospheric conditions which took ca. 10 minutes and then the drug loaded 96-microwell plate was placed in the incubator programmed to attain 1.5% oxygen concentration. The incubator takes ca. 30-40 minutes to reach the 1.5% oxygen level.

DNA interaction Studies

Preparation of Stock DNA solution. A concentrated stock solution of CT DNA was prepared in 50mM Tris-NaCl solution at pH 7.4 which showed two absorption bands at 260nm and 280nm and their absorption ratio was 1.9, indicating that the DNA was apparently free from protein[9] and the concentration of the DNA was determined from the absorption value at 260 nm (Molar extinction coefficient is 6600 $dm^3mol^{-1}cm^{-1}$)[10]. The stock solution of the DNA was stored at 4°C and used within four days.

Binding studies with CT DNA. Interaction of **1** with CT DNA was measured with the help of UV-vis spectroscopy in tris buffer–DMF (9 : 1) media (v/v). The stock solution of the complex was made in DMF. Spectroscopic titrations were carried out at room temperature (25°C). The concentration of **1** for the binding experiments was fixed to 5×10^{-5} M. The

change in the absorbance was monitored with subsequent addition of an aliquot of 10 μL (concentration of 5×10^{-4} M) of CT DNA in the sample and reference cuvette. The spectra were recorded after equilibration of the mixture for 5 min after each addition. The titration was continued until there was no significant change in absorbance for at least three successive additions.

Hydrolysis study. The hydrolysis studies of complex **1** were measured by UV-Vis absorption spectroscopy at two different pH 7.4 and 6.7 (using 1% acetonitrile-20 mM phosphate buffer in 40 mM or 4 mM NaCl) for 2 hours. The hydrolysis study was also performed in 1% acetonitrile water mixture. For all the reactions the corresponding equilibrium constants were determined from the equation of pseudo first order rate equation as shown below,

$$[A] = [A_o]e^{-kt}$$

$$\text{or, } \log([A_o]/[A]) = kt/2.303$$

Where, $[A_o]$ and $[A]$ are the initial absorbance and absorbance at time t respectively, k is the equilibrium rate constant. Hence from the slope of the plot of $\log([A_o]/[A])$ vs t we determine the equilibrium rate constant or hydrolysis rate constant. The half lives were calculated from the following equation,

$$t_{1/2} = 0.6931 / k$$

Hydrolysis of complex **1** was also monitored by ^{1}H NMR by taking spectra at different interval of time in DMSO-d_6 and D_2O mixture at 25°C (7:3 v/v) and the conversion was determined from the integration of ^{1}H NMR spectra.

Cell cycle analysis. MCF-7 cells, 5×10^5 per plate, were seeded in a 100 mm dia Petri dish in 12 mL DMEM and incubated at 37°C in a 5% carbon dioxide atmosphere. After 48 h, media was removed and fresh media was added. Then adequate concentrations of complex solutions were added and incubated at previously described culturing condition. After 24 h of drug

exposure, cells were harvested by trypsinization, washed twice with cold 1X PBS (pH 7.2). Cell fixing was done by keeping a 70% aqueous cell solution at 4°C for 12 h. DNA staining was performed by resuspending the cell pellets in 1X PBS solution comprising of PI (55 μg/mL) and RNase A (100 μg/mL) solution. The cell suspension was gently mixed and incubated at 37°C for half an hour in dark. Samples were analyzed in a BD Biosciences FACS Calibur flow cytometer.

DNA Ladder Assay for Apoptosis Detection. Cellular apoptosis induced by complex **1** was detected using DNA ladder assay,[11] where 5×10^5 MCF-7 cells were seeded in each 100 mm tissue culture petri dish and incubated for 48 hours in DMEM at 37°C. After that media was removed and fresh media was added. The cells were then treated with required concentration of complex solution and again incubated for another 24 hours followed by which they were harvested by trypsinization and centrifuged at 2000 rpm for 5 minutes. Then after washing with 1X PBS (pH = 7.2), the cells were resuspended in 500 μL lysis buffer (20 mM Tris-HCl (pH 7.4), 0.4 mM EDTA, 0.25% Triton-X 100) and incubated for 15 minutes at room temperature. Lysed cells were centrifuged at 14000 rpm for 10 minutes. The supernatant solution was collected, mixed with 1:1 (v/v) phenol-chloroform mixture (1 mL) and the aqueous layer was removed carefully. Then 55 μL of 5 M NaCl and 500 μL isopropanol were added respectively. The resultant mixture was incubated for overnight at -20°C. After that the solution was centrifuged at 14000 rpm and washed with 70% ice cold ethanol and dried in air which was again resuspended in 1X TE solution (10 mM Tris-HCl (pH 8.0), 1 mM EDTA) containing RNase (150 μg/mL) and then it was incubated at 37°C for 20 minutes. The supernatant was mixed with bromophenol blue dye and loaded in 1.6% agarose gel containing EtBr (1.0 μg/mL) and run at 60 V for around 3 h in 1X TBE (Tris-borate-EDTA) buffer. After that the picture of the gel was taken through gel documentation system of Bio-Rad and from the known base pair ladder, the bands were identified.

Optical Microscopy Imaging. The optical microscopy image of MCF-7 were taken by using OLYMPUS IX 81 epifluorescence inverted microscope at 60X magnification after 24 hours incubation with specific concentration of respective complex and DAPI was used as a fluorescent nuclear staining dye. OLYMPUS Cell P software was used to process and acquire DIC and fluorescence microscopy images.

Binding studies with reduced L-glutathione (GSH). The binding of complex **1** with reduced L-glutathione was performed by ^{1}H NMR after degassing a D_2O/ DMSO-d_6 (7:3 v/v) mixture at 25°C under nitrogen atmosphere to minimize the auto oxidation process. The experiment involved 0.002 mmol of **1** and 0.04 mmol (20 equiv.) of GSH dissolved in the solution. The binding was studied upto 24 hours at different interval of time.

Stability in saline solution. The stability of complex **1** in 110 mM saline solution, D_2O: DMSO-d_6 (7:3 v/v) was observed by ^{1}H NMR at 25°C to probe the stability outside the cell where Cl^- concentration is higher. 2 mg of **1** was dissolved in 600 µL of 7:3 D_2O/DMSO-d_6 solution containing 3.5 mg of NaCl and the spectra were recorded upto ten days.

Statistical Analysis. All the IC_{50} data are given are mean ± standard deviation. The results are mean of three independent experiments carried out in each cell line where, in each experiment each concentration was assayed in triplicate. The statistical analyses were performed using Graph pad prism® software 5.0 with student's t-test.

Table S1. Crystal Data, Data Collection and Refinement Parameters

	1
Empirical formula	$C_{26}H_{35}ClF_6N_3PRu$
Formula weight	671.06
Temperature (K)	100(2)
Wavelength(Å)	0.71073
Crystal system	Monoclinic
space group	$P2_1/n$
a (Å)	17.370(2)
b (Å)	10.0067(12)
c (Å)	17.554(2)
α (deg.)	90
β (deg.)	110.743(2)
γ (deg.)	90
Volume (Å^3)	2853.3(6)
Z, Calculated density (Mg/m^3)	4, 1.585
F(000)	1380
Reflections collected / unique	43861 / 7041 [R(int) = 0.0575]
Max. and min. transmission	0.893 and 0.659
Goodness-of-fit on F^2	1.055
Final R indices [$I>2\sigma$(I)]	[a]R_1 = 0.0422, [b]wR_2 = 0.1040
R indices (all data)	[a]R_1 = 0.0574, [b]wR_2 = 0.1144

[a]$R_1 = \Sigma|F_o| - |F_c||/\Sigma|F_o|$. [b]$wR_2 = [\Sigma[w(F_o^2 - F_c^2)^2]/ \Sigma w(F_o^2)^2]^{1/2}$

Table S2. Selected bond lengths (Å) and angles (°) for complex **1.**

1			
Ru(1)-N(2)	2.083(3)	N(2)-Ru(1)-N(1)	75.99(10)
Ru(1)-N(1)	2.134(2)	N(2)-Ru(1)-C(17)	150.93(12)
Ru(1)-C(19)	2.177(3)	N(2)-Ru(1)-C(18)	168.18(11)
Ru(1)-C(21)	2.181(3)	N(2)-Ru(1)-C(19)	130.69(11)
Ru(1)-C(22)	2.193(3)	N(2)-Ru(1)-C(20)	101.91(11)
Ru(1)-C(18)	2.212(3)	N(2)-Ru(1)-C(21)	95.83(11)
Ru(1)-C(20)	2.225(3)	N(2)-Ru(1)-C(22)	116.02(11)
Ru(1)-C(17)	2.243(3)	N(2)-Ru(1)-Cl(1)	81.13(7)
Ru(1)-Cl(1)	2.3790(8)	N(1)-Ru(1)-Cl(1)	88.02(6)

Table S3. Rate of hydrolysis, half-life and IC_{50} values of Ru^{II}-arene halide complexes. Only those complexes are tabulated for which the both the hydrolysis and cytotoxicity data are available.

Sl. No.	Complex	Rate k (h^{-1})[a]	$t_{1/2}$ (h)	IC_{50} (cell line), μM	Ref.
1	[(η^6-*p*-cymene)Ru(azpy-NMe_2)I]PF_6	No Hyd[c]	-	4 (A2780), 3 (A549)	12
2	[(η^6-*p*-cymene)Ru(azpy-OH)I]PF_6	No Hyd[c]	-	4 (A2780, A549)	
3	[(η^6-biphenyl)Ru(azpy-NMe_2)I]PF_6	No Hyd[c]	-	3 (A2780), 2 (A549)	
4	[(η^6-biphenyl)Ru(azpy-OH)I]PF_6	No Hyd[c]	-	5 (A2780), 6 (A549)	
5	[(η^6-*p*-cymene)Ru(azpy)I]PF_6	No Hyd[c]	-	>100 (A2780, A549)	
6	[Ru(η^6-C_6Me_6)(ptn)Cl]Cl	No Hyd[e]	-	203 ± 5 (A2780)	13
7	[(η^6-*p*-cym)RuCl(imidazole-CO_2H)(PPh_3)]-Octreotide conjugate	No Hyd[d]	-	63.00 ± 1.53 (MCF-7), 26 ± 2 (DU-145), 45.17 ± 2.61 (CHO)	14
8	[Bromido{3-(oxo-κO)-2-phenyl-chromen-4(1H)-onato-κO}-(η^6-*p*-cymene) ruthenium(II)]	No Hyd[t]	-	27 ± 4 (A549), 2.8 ± 0.4 (CH1), 12 ± 1 (SW 480)	15
9	[Iodido{3-(oxo-κO)-2-phenyl-chromen-4(1H)-onato-κO}4-(η^6-*p*-cymene) ruthenium(II)]	No Hyd[t]	-	16 ± 1 (A549), 1.6 ± 0.2 (CH1), 9.6 ± 1.5 (SW 480)	
10	[Chlorido{3-(oxo-κO)-2-phenyl-chromen-4(1H)-onato-κO}-(η^6-toluene) ruthenium(II)]	No Hyd[t]	-	19 ± 1 (A549), 3.2 ± 0.1 (CH1), 12 ± 3 (SW 480)	
11	[Chlorido{3-(oxo-κO)-2-phenyl-chromen-4(1H)-onato-κO}-(η^6-biphenyl) ruthenium(II)]	No Hyd[t]	-	28 ± 5 (A549), 5.5 ± 1.2 (CH1), 9.2 ± 1.9 (SW 480)	
12	[Ru(η^6-*p*-cymene)(ptn)Cl]Cl	>168[e]	-	278 ± 12 (A2780)	13
13	[Ru(η^6-C_6H_6)(ptn)Cl]Cl	>168[e]	-	179 ± 8 (A2780)	
14	((η^6-*p*-cym)$RuCl_2$(1-(2,3,4,6-tetra-O-acetyl-*β*-D-glucopyranosyl)-4-methyl-5-phenyl-1H-1,2,3-triazole)	>168[f]	-	41.0 ± 8.2 (A2780), >200 (A2780R), >200 (HEK)	16
15	[chlorido{3-(oxo-κO)-2-phenyl-chromen-4(1H)-onato-κO}(η^6-*p*-cymene) ruthenium(II)]	144[t]	-	20 ± 2 (A549), 2.1 ± 0.2 (CH1), 9.6 ± 1.5 (SW 480)	17-18
16	[chlorido{3-(oxo-κO)-2-(4-fluorophenyl)-chromen-4(1H)-onato-κO}(η^6-*p*-cymene) ruthenium(II)]	144[t]	-	18 ± 1 (A549), 1.7 ± 0.4 (CH1), 7.9 ± 2.1 (SW 480)	
17	[chlorido{3-(oxo-κO)-2-(4-chlorophenyl)-chromen-4(1H)-onato-κO}(η^6-*p*-cymene) ruthenium(II)]	144[t]	-	9.5 ± 0.5 (A549), 0.86 ± 0.06 (CH1), 3.8 ± 0.5 (SW 480)	
18	[Ru(η^6-$C_6H_5CH_3$)(ptn)Cl]Cl	>24[e]	-	154 ± 11 (A2780)	13
19	Chlorido(η^6-*p*-cymene)(ofloxacinato-κ^2O,O)ruthenium(II)	<18[l]	-	>320 (A549), 18 ± 7 (CH1), 225 ± 39 (SW 480)	19
20	Chlorido(η^6-*p*-cymene)(nalidixicato-κ^2O,O)ruthenium(II)	<18[l]	-	>320 (A549, CH1, SW 480)	
21	Chlorido(η^6-*p*-cymene)(cinoxacinato-κ^2O,O)ruthenium(II)	<18[l]	-	>320 (A549, CH1, SW 480)	
22	[(η^6-*p*-cym)Ru(azpy-OH)Cl][PF_6]	0.033[g]	21.03	58 (A2780), >100 (A549)	20
23	[(η^6-bip)Ru(azpy-NMe_2)Cl][PF_6]	0.034[g]	20.27	44 (A2780), 49 (A549)	
24	[(η^6-bip)Ru(azpy-OH)Cl][PF_6]	0.053[g]	13.05	18 (A2780), 56 (A549)	
25	[(η^6-bip)Ru(bpm)I][PF_6]	0.0583[i]	11.91	>100 (A2780)	21

26	Dichlorido(η^6-*p*-cymene)(3,5,6-bicyclophosphite-ethyl-1-thio-α-D-glucofuranoside) ruthenium(II)	0.096[j]	11.58	>700 (A2780, A2780 cisR, A549, HCEC, LNZ 308, Me 300), 93 ± 26 (CH1), 500 ± 100 (SW 480)	22
27	[(η^6-*p*-cym)Ru(azpy)Cl][PF_6]	0.0601[h]	11.55	>100 (A2780, A549)	20
28	[(η^6-*p*-cym)Ru(azpy-NMe_2)Cl][PF_6]	0.078[g]	8.90	>100 (A2780, A549)	
29	[(η^6-bip)Ru(azpy)Cl] [PF_6]	0.0782[h]	8.87	>100 (A2780, A549)	
30	[(η^6-*p*-cym)Ru(bpm)I][PF_6]	0.177[i]	3.92	>100 (A2780)	21
31	[(η^6-bip)Ru(bpm)Cl][PF_6]	0.236[i]	2.94	>100 (A2780)	
32	[Ru(η^6-*p*-cymene)Cl_2(PTA)	<0.25[u]	-	353 (A2780), 252 (A2780 cisR)	23
33	Ru(pta)(η^6-$C_6H_5CF_3$)Cl_2	0.254[b,k]	2.73	38 (A2780)	24
34	[(η^6-*p*-cym)Ru(azpyz-NMe_2)Cl] [PF_6]	0.3233[h]	2.14	18 (A2780), 41 (A549)	20
35	[(η^6-*p*-cym)Ru(bpm)Cl][PF_6]	0.451[i]	1.54	>100 (A2780)	21
36	[(η^6-thn)Ru(bpm)Cl][PF_6]	0.463[i]	1.50	>100 (A2780)	
37	Dichlorido(η^6-*p*-cymene)(3,5,6-bicyclophosphite-N-acetyl-α-D-glucofuranosylamine)ruthenium(II)	0.54[j]	1.43	153 ± 13 (CH1), 430 ± 35 (SW 480)	22
38	Dichlorido(η^6-*p*-cymene)(3,5,6-bicyclophosphite-1,2-*O*-cyclohexylidene-α-D-glucofuranoside) ruthenium(II)	0.582[j]	1.13	351 ± 89 (A2780), 374 ± 93 (A2780 cisR), 223 ± 14 (A549), 29 ± 4 (CH1), 506 ± 62 (HCEC), 212 ± 54 (LNZ 308), 327 ± 55 (Me 300), 150 ± 19 (SW 480)	
39	[(η^6-*p*-cym)Ru(phendio)Cl][PF_6]	0.696[i]	1.00	ND	21
40	(η^6-C_6H_6)RuCl(($3,5$-$(CF_3)_2C_6H_3NC(CH_3)$)$_2$ CH)	<1[m]	-	91 ± 3 (A2780), 108 ± 3 (A2780 cisR)	25
41	(η^6-C_6H_6)RuCl(($2,6$-$(CH_3)_2C_6H_3NC(CF_3)$)$_2$ CH)	<1[m]	-	1.8 ± 0.3 (A2780), 1.9 ± 0.5 (A2780 cisR)	
42	(η^6-C_6H_6)RuCl(($3,5$-$(CF_3)_2C_6H_3NC(CF_3)$)$_2$ CH)	<1[m]	-	<0.5 (A2780, A2780 cisR)	
43	Dichlorido(η^6-*p*-cymene)(3,5,6-bicyclophosphite-1,2-*O*-isopropylidene-α-D-glucofuranoside)ruthenium(II)	0.702[j]	1.02	504 ± 56 (A2780), 678 ± 80 (A2780 cisR), 498 ± 17 (A549), 60 ± 14 (CH1), >700 (HCEC), 575 ± 25 (LNZ 308), 617 ± 13 (Me 300), 361 ± 122 (SW 480)	22
44	[(η^6-benene)RuCl([1-(2-pyridyl)-β-carboline])][PF_6]	0.956[n]	0.72	50.4 ± 4.1 (A549), 28.3 ± 3.4 (A549 cisR), 76.3 ± 5.5 (CNE-2), 44.3 ± 3.7 (HeLa), 61.2 ± 4.9 (HepG2), >200 (HLF)	26
45	[(η^6-ind)Ru(bpm)Cl][PF_6]	0.96[i]	0.72	>100 (A2780)	21
46	[(η^6-*p*-cym)RuCl([1-(2-pyridyl)-β-carboline])][PF_6]	0.985[n]	0.70	40.6 ± 2.8 (A549), 23.4 ± 1.8 (A549 cisR), 16.9 ± 1.4 (CNE-2), 16.3 ± 1.5 (HeLa), 37.7 ± 3.6 (HepG2), >200 (HLF)	26
47	[(η^6-bip)Ru(bpm)Br][PF_6]	1.03[i]	0.67	>100 (A2780)	21
48	[(η^6-hmb)Ru(bpm)Cl][PF_6]	1.032[i]	0.67	>100 (A2780)	
49	[(η^6-bz)Ru(en)I][PF_6]	1.058[o]	0.66	20 (A2780)	27-28
50	[(η^6-bip)Ru(en)I][PF_6]	1.156[o]	0.60	5 (A2780)	27
51	[(η^6-*p*-cym)Ru(N-2,4,6-trimethyl-Ph-picolinamide)Cl][PF_6]	1.63[p]	0.43	>50 (A2780, A2780 cisR, HCT116)	29
52	[(η^6-*p*-cym)Ru(phen)Cl][PF_6]	1.83[i]	0.38	22.9 (A2780)	21
53	[(η^6-ind)Ru(en)I][PF_6]	1.843[o]	0.38	ND	27
54	[(η^6-*p*-cym)Ru(bpm)Br][PF_6]	1.86[i]	0.37	>100 (A2780)	21
55	[(η^6-*p*-cym)Ru(bathophen)Cl][PF_6]	2.448[i]	0.28	0.5 (A2780)	
56	[(η^6-*p*-cymene)RuCl(κ^2-N,N-2-pydaT)](BF_4)	2.7[q]	0.26	8.60 ± 0.20 (A2780)	30-31

57	[(η^6-bip)Ru(bipy(OH)O)Cl]	2.778[r]	0.25	40 ± 8 (A2780), >100 ± 9 (A549)	32
58	[(η^6-etb)Ru(bpm)Cl][PF_6]	3[i]	0.24	ND	21
59	[(η^6-*p*-cym)Ru(en)I][PF_6]	3.413[o]	0.20	9 (A2780)	27-28
60	[(η^6-bip)Ru(en)Br][PF_6]	3.78[o]	0.18	ND	27
61	[(η^6-bip)Ru(en)Cl][PF_6]	4.464[o]	0.16	5 (A2780)	27-28
62	[(η^6-ind)Ru(phen)Cl][PF_6]	4.506[r]	0.15	52 (A2780)	32-33
63	[(η^6-bz)Ru(en)Br][PF_6]	5.4[o]	0.13	ND	27
64	[(η^6-thn)Ru(bipy(OH)O)Cl]	5.508[r]	0.13	7 ± 1 (A2780), 24 ± 4 (A549)	32
65	[(η^6-hmb)Ru(*o*-bqdi)Cl]Cl	5.55[s]	0.12	>100 (A2780, A549)	34
66	[(η^6-bip)Ru(bipy)Cl][PF_6]	5.598[r]	0.12	>100 ± 10 (A2780)	32-33
67	[(η^6-*p*-cym)Ru(N-2,4-difluoro-Ph-picolinamide)Cl]	≥5.9[p]	≤0.12	>50 (A2780, A2780 cisR)	29
68	[(η^6-ind)Ru(4,4′-Me_2-bipy)Cl][PF_6]	6.78[r]	0.10	>100 (A2780)	32-33
69	[(η^6-bz)Ru(en)Cl][PF_6]	7.128[o]	0.10	17 (A2780)	27-28
70	[(η^6-ind)Ru(bipy)Cl][PF_6]	7.26[r]	0.10	>100 (A2780)	32-33
71	[(η^6-ind)Ru(en)Br][PF_6]	7.776[o]	0.09	ND	27
72	[(η^6-dha)Ru(en)Cl][PF_6]	8.028[o]	0.09	2 (A2780)	27-28
73	[(η^6-benzene)RuCl([1-(2-imidazolyl)-β-carboline])][PF_6]	8.15[n]	0.09	15.8 ± 1.5 (A549), 2.9 ± 0.3 (A549 cisR), 2.1 ± 0.3 (CNE-2), 5.9 ± 0.9 (HeLa), 10.8 ± 0.9 (HepG2), 78.3 ± 6.9 (HLF)	26
74	[Bromido{3-(oxo-κO)-2-(4-chlorophenyl)-chromen-4(1H)-onato-κO}(η^6-*p*-cymene)ruthenium(II)]	>0.083[t]	-	7.9 ± 0.6 (A549), 0.86 ± 0.04 (CH1), 3.4 ± 0.4 (SW 480)	15
75	[Iodido{3-(oxo-κO)-2-(4-chlorophenyl)-chromen-4(1H)-onato-κO}-(η^6-*p*-cymene) ruthenium(II)]	>0.083[t]	-	8.9 ± 0.8 (A549), 1.2 ± 0.3 (CH1), 4.7 ± 0.9 (SW 480)	
76	[Chlorido{3-(oxo-κO)-2-(4-chlorophenyl)-chromen-4(1H)-onato-κO}(η^6-toluene) ruthenium(II)]	>0.083[t]	-	7.8 ± 2.5 (A549), 0.88 ± 0.17 (CH1), 4.7 ± 0.6 (SW 480)	
77	[Chlorido{3-(oxo-κO)-2-(4-chlorophenyl)-chromen-4(1H)-onato-κO}(η^6-biphenyl) ruthenium(II)]	>0.083[t]	-	59 ± 1 (A549), 6.3 ± 1.1 (CH1), 21 ± 4 (SW 480)	
78	[Chlorido{3-(oxo-κO)-2-phenyl-quinolon-4(1H)-onato-κO}-(η^6-*p*-cymene) ruthenium(II)]	>0.083[t]	-	17 ± 2 (A549), 4.0 ± 0.2 (CH1), 14 ± 1 (SW 480)	
79	[Chlorido{3-(oxo-κO)-1-methyl-2-phenyl-quinolon-4(1H)- onato-κO}(η^6-*p*-cymene) ruthenium(II)]	>0.083[t]	-	19 ± 1 (A549), 5.3 ± 0.2 (CH1), 12 ± 2 (SW 480)	
80	[(η^6-ind)Ru(en)Cl][PF_6]	8.244[o]	0.08	8 (A2780)	27
81	[(η^6-*p*-cym)RuCl([1-(2-imidazolyl)-β-carboline])][PF_6]	8.49[n]	0.08	5.4 ± 0.5 (A549), 1.9 ± 0.3 (A549 cisR), 1.5 ± 0.2 (CNE-2), 2.4 ± 0.2 (HeLa), 7.5 ± 0.8 (HepG2), 44.1 ± 4.7 (HLF)	26
82	[(η^6-tha)Ru(en)Cl][PF_6]	8.496[o]	0.08	0.5 (A2780)	27-28
83	[(η^6-ind)Ru(bipy(OH)O)Cl]	9.876[r]	0.07	18 ± 3 (A2780), 39 ± 5 (A549)	32
84	[(η^6-bip)Ru(NH_3)Cl_2]	33.3[v]	0.02	>100 (A2780)	35
85	[(η^6-*p*-cym)Ru(NH_3)Cl_2]	43.2[v]	0.02	>100 (A2780)	

86	[(η^6-*p*-cymene)Ru^{II}(Cl)(2-methylpyrone)]	<1 sec[w]	-	>100 (CH1, SW480)	36
87	[(η^6-*p*-cymene)Ru^{II}(Cl)(2-methylthiopyrone)]	<1 sec[w]	-	13 ± 4 (CH1), 5.1 ± 0.5 (SW 480)	
88	[(η^6-*p*-cymene)Ru^{II}(Cl)(6-methylpyrone)]	<1 sec[w]	-	239 ± 22 (CH1), 359 ± 119 (SW 480)	
89	[(η^6-*p*-cymene)Ru^{II}(Cl)(6-methylthiopyrone)]	<1 sec[w]	-	35 ± 8 (CH1), 20 ± 7 (SW 480)	

ptn; 7-phospha-1,3,5-triazatricyclo[3.3.1.1]decane , hmb; hexamethylbenzene, ind; indane, thn; 1,2,3,4-tetrahydronaphthalene, phen; 1,10-phenanthroline, phendio; 1,10-phenanthroline-5,6-dione, bathophen; 4,7-diphenyl-1,10-phenanthroline. p-cym; p-cymene, bpm; 2,2´-bipyrimidine, etb; ethyl benzoate ,bip; biphenyl, bipy; bipyridine. ND indicate not determine.

[a] the esd values of reported rate of hydrolysis is not taken into account, < indicate hydrolysis complete or some percentage of hydrolysis takes place within the time, > indicate hydrolysis starts after the mentioned time. ; [b] First aquation rate was considered; [c] 10mM phosphate buffer (containing 95% D_2O/5% MeOD, pH 7.3) and at 310 K by ^1H NMR spectroscopy; [d] 4mM NaCl, 310 K by reverse phase HPLC together with MS upto 24h; [e] 5 mM NaCl, 1% v/v DMSO in D_2O by ^1H NMR spectroscopy; [f] 10 mM phosphate buffer, pH 7.4 by UV-vis spectroscopy; [g] 90% H_2O, 10% D_2O at 310 K by ^1H NMR spectroscopy; [h] 95% H_2O, 5% MeOH at 310 K by UV-vis spectroscopy; [i] 5 % MeOH/95 % H_2O at 310K by UV-vis spectroscopy; [j] 20 mm phosphate buffer H_2O/D_2O (9/1) (pH 7.4) by ^1H NMR spectroscopy; [k] unbuffered pH 5.7 in D_2O by ^1H NMR spectroscopy; [l] D_2O, 298K by ^1H NMR spectroscopy; [m] by UV-vis spectroscopy and ^1H NMR spectroscopy ; [n] H_2O, 298K by UV-vis spectroscopy; [o] 19:1mixtures of water and methanol at 298 K by UV-vis spectroscopy; [p] 5% MeOD-d_4/95% D_2O mixture was monitored by ^1H NMR at 288 K; [q] water by UV-vis spectroscopy; [r] 95% H_2O, 5% MeOH, 310K by UV-vis spectroscopy; [s] water, 310K by UV-vis spectroscopy; [t] 10% (v/v) d_6-DMSO/D_2O by ^1H NMR spectroscopy; [u] 10 mM phosphate buffer pH 7.4 by UV-vis spectroscopy; [v] D_2O or 5% MeOH/95% H_2O, at 310K by UV-vis spectroscopy; [w] D_2O or 10% DMSO-d_6/90% D_2O by ^1H NMR spectroscopy.

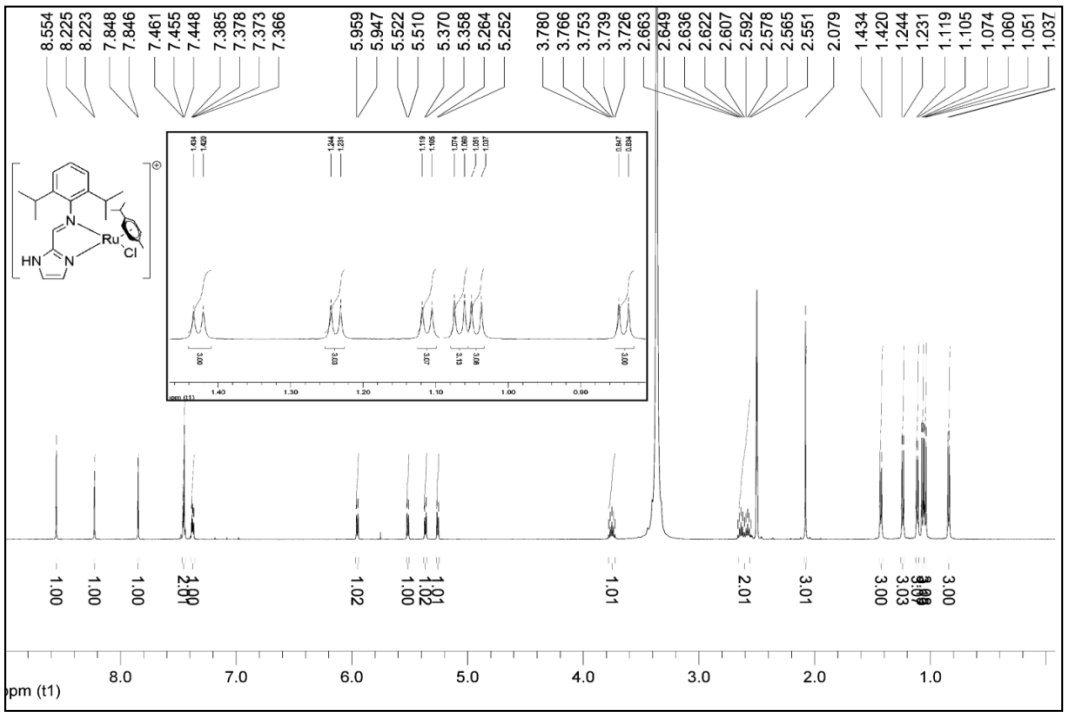

Fig. S1 ^{1}H NMR spectrum of complex **1** in DMSO-d_6

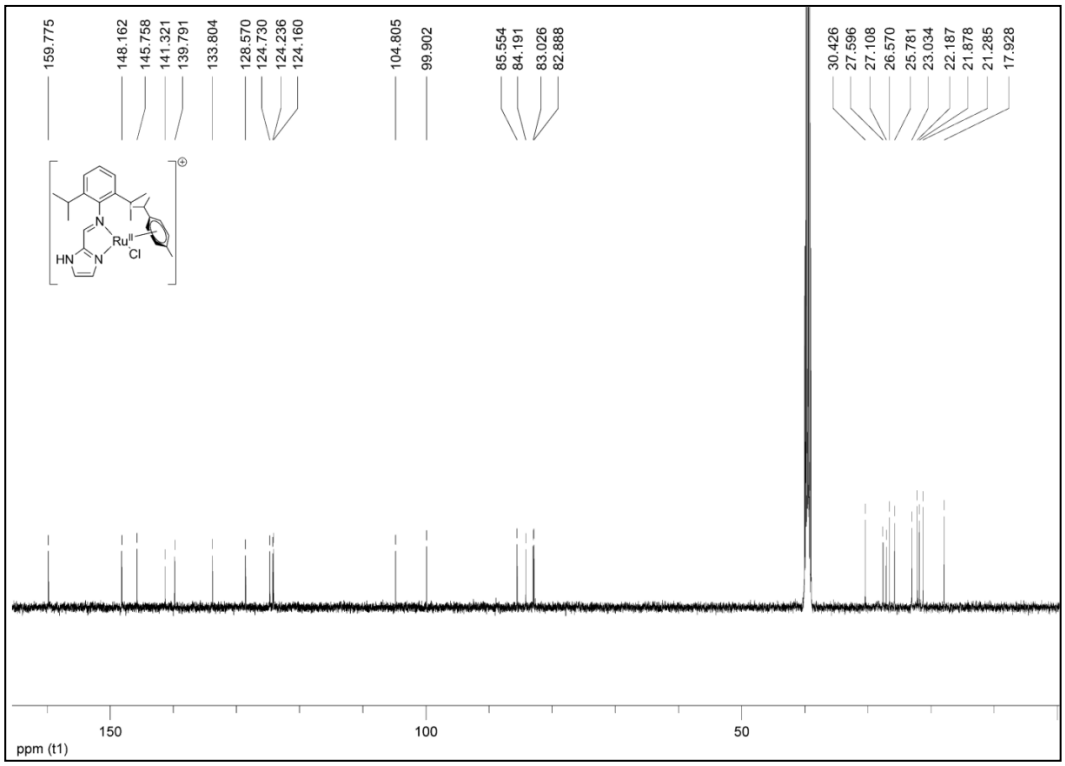

Fig. S2 ^{13}C NMR of **1** in DMSO-d_6

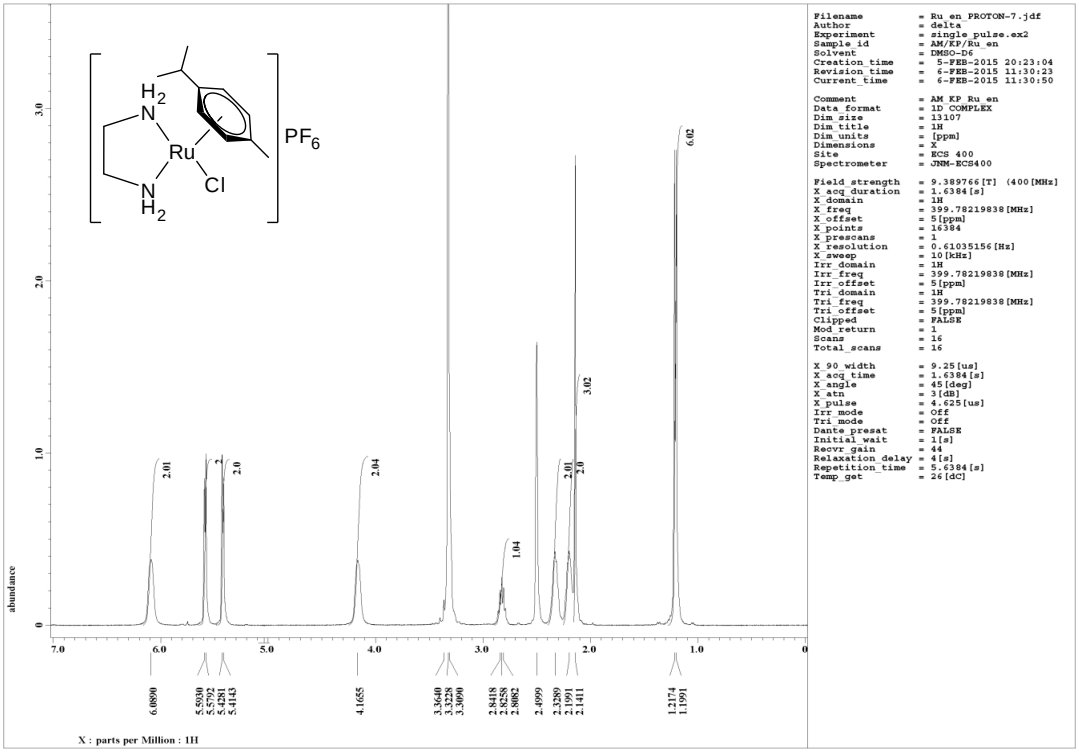

Fig. S3 ^{1}H NMR spectrum of complex **C1** in DMSO-d_6.

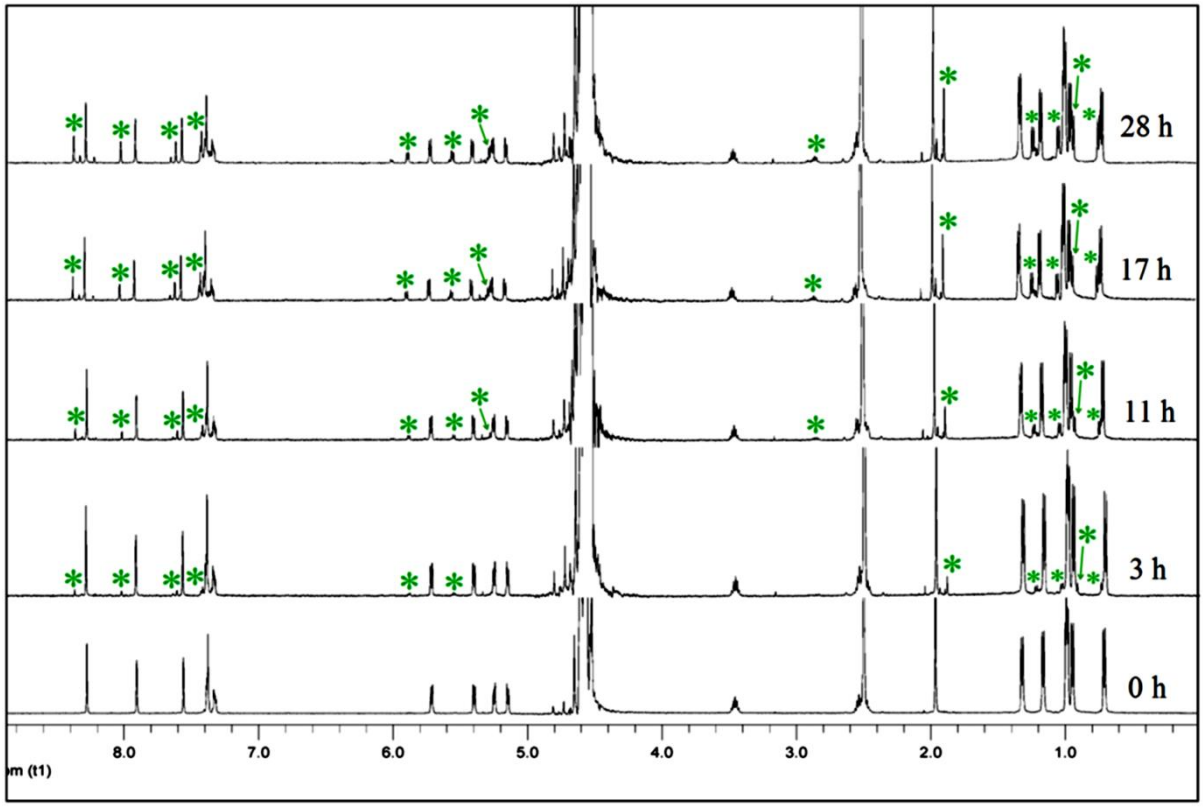

Fig. S4 Hydrolysis study of complex **1** in 3:7 v/v DMSO-d_6 and D_2O mixture measured by ^{1}H NMR with time at 25°C. * indicate the peak corresponding to the hydrolysis product.

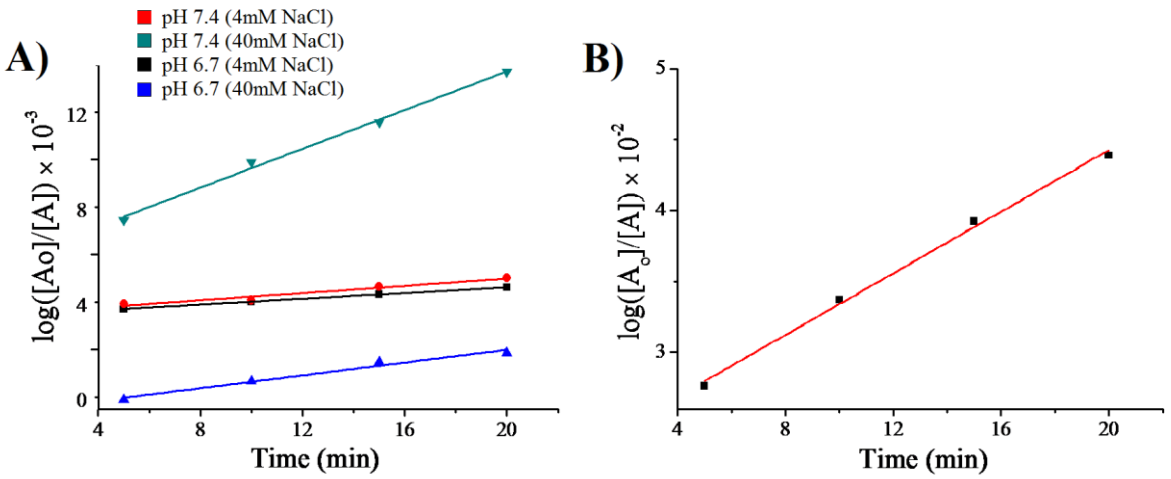

Fig. S5 A) log([A_o]/[A]) vs time (min) plot for the hydrolysis of **1** in 1% acetonitrile, aqueous buffer solution of two different pH (7.4, 6.7) measured by UV-visible spectroscopy in presence of 4 and 40 mM NaCl. B) log([A_o]/[A]) vs time (min) plot for the hydrolysis of **1** in 1% acetonitrile-water mixture. The plots provided are for one independent experiment out of the three (for A) or two (for B) independent experiments performed.

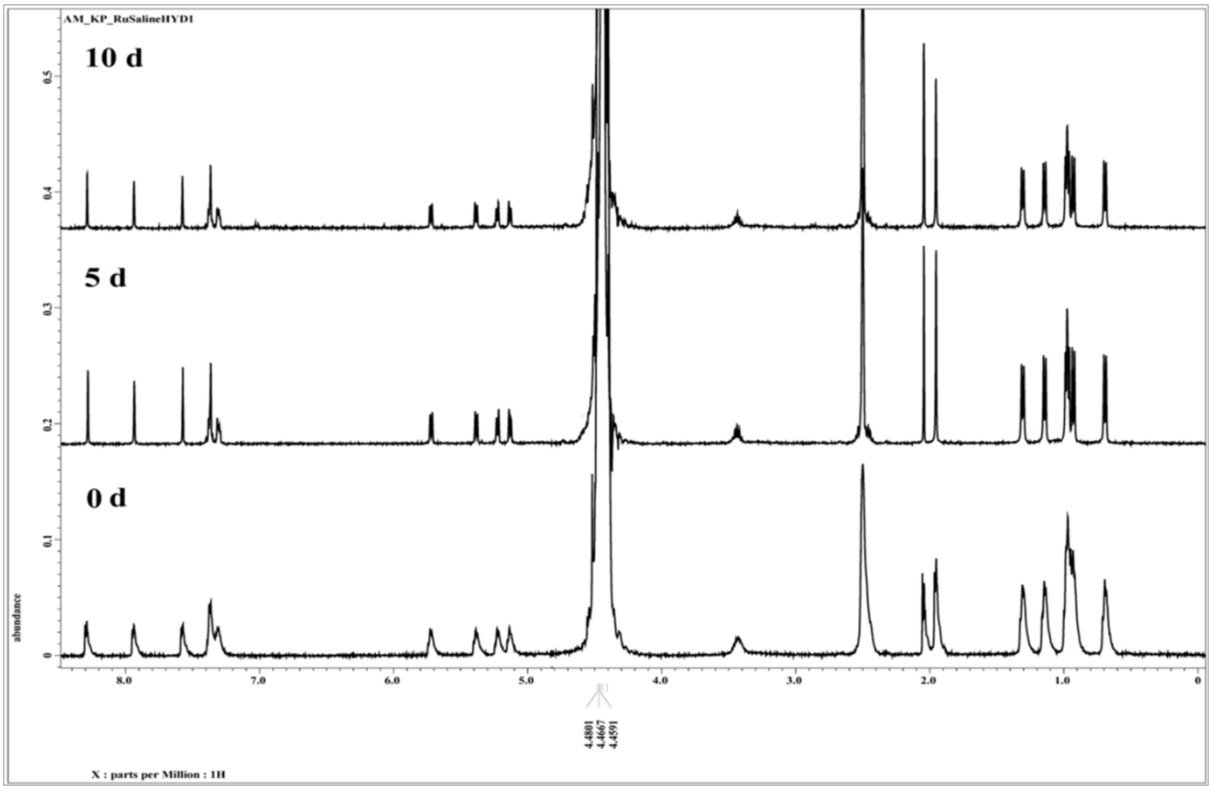

Fig. S6 ^{1}H NMR spectra of complex **1** in 110 mM NaCl solution in 30% DMSO-d_6 in D_2O mixture, recorded at different interval of time at 25°C. t = 0 d, stands for the spectra recorded immediately after dissolving complex **1**.

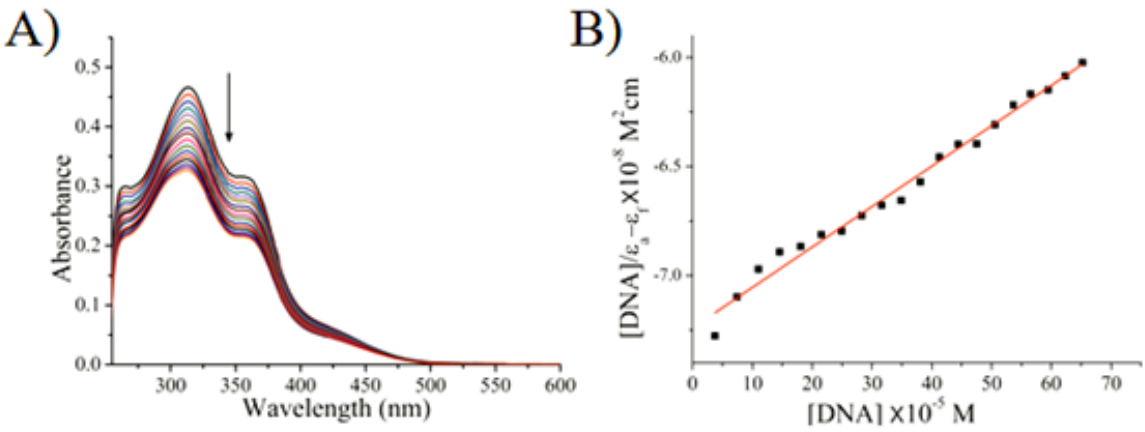

Fig. S7 A) Absorption spectral change upon addition of CT DNA solution to the solution of **1** in Tris-NaCl/DMF (9:1) at pH 7.4 (temperature 25 °C). B) The plot of [DNA]/ (ε_a - ε_f) vs [DNA] for complex **1** to calculate apparent binding constant (K_b). The plots provided are for one independent experiment out of the three independent experiments performed.

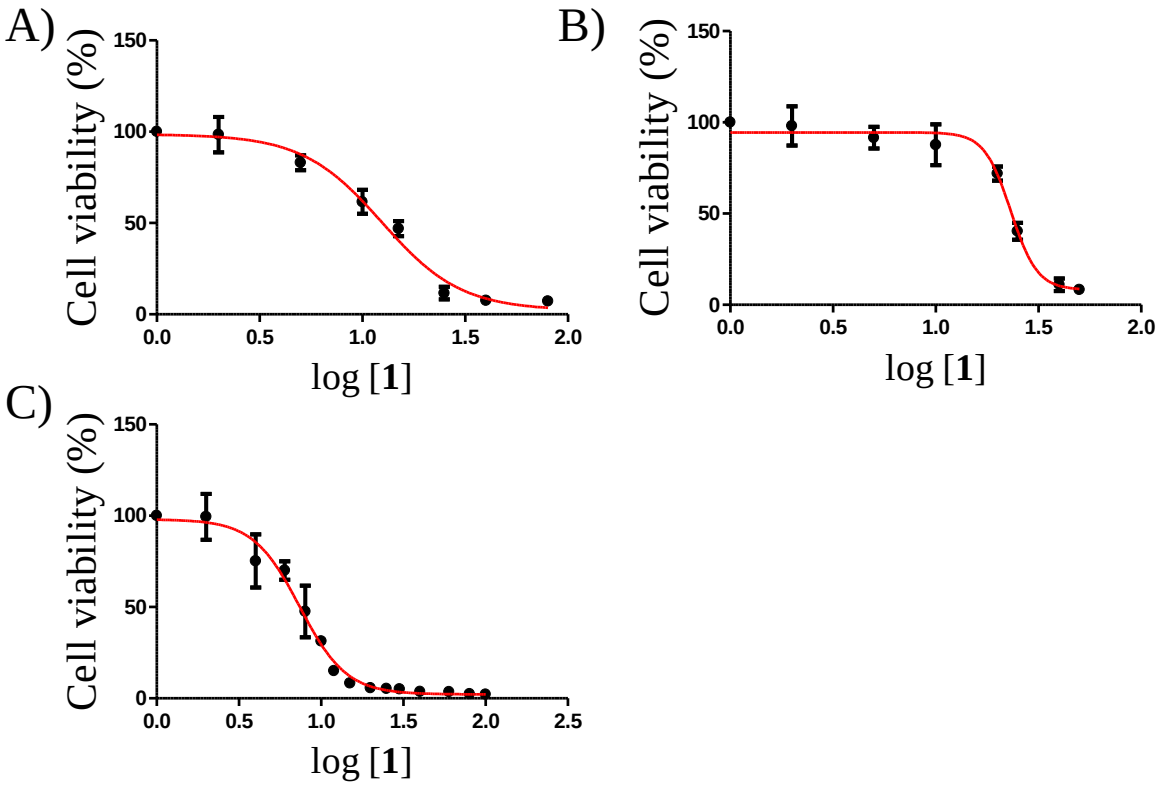

Fig. S8 Plots of cell viability (%) vs. log of concentration for **1** A) MCF-7, B) A549 and C) HeLa cell lines after incubation for 48 h determine from MTT assays under normoxic condition. The plots provided are for one independent experiment out of the three independent experiments performed with each concentration.

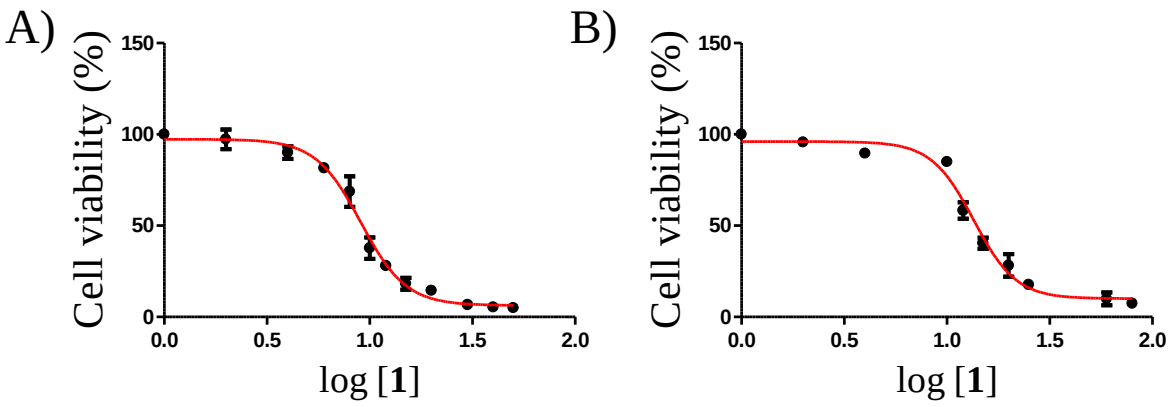

Fig. S9 Plots of cell viability (%) vs. log of concentration for **1** A) MCF-7, B) A549 cell lines after incubation for 48 h determine from MTT assays under hypoxic condition. The plots provided are for one independent experiment out of the three independent experiments performed with each concentration.

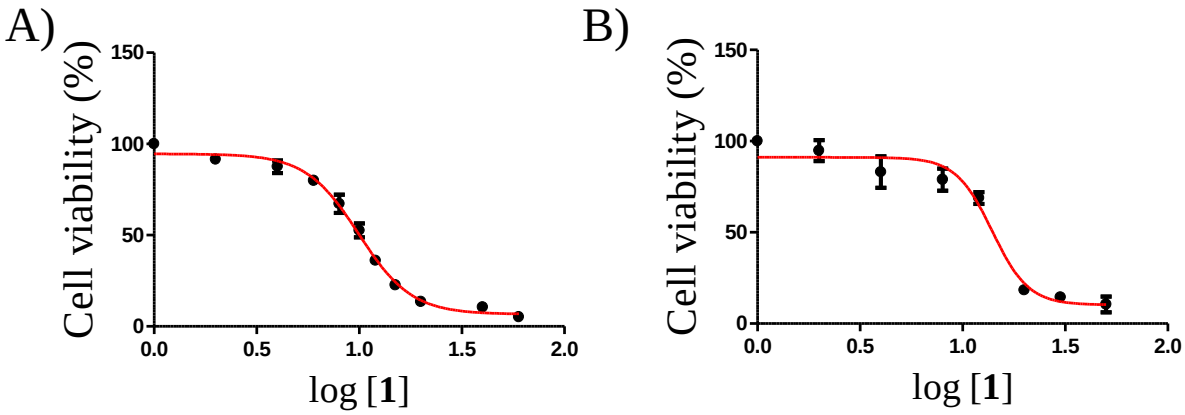

Fig. S10 Plots of cell viability (%) vs. log of concentration for **1** A) MCF-7, B) A549 cell lines after incubation for 48 h determine from MTT assays under hypoxic condition in presence of 1 mM L-glutathione. The plots provided are for one independent experiment out of the three independent experiments performed with each concentration.

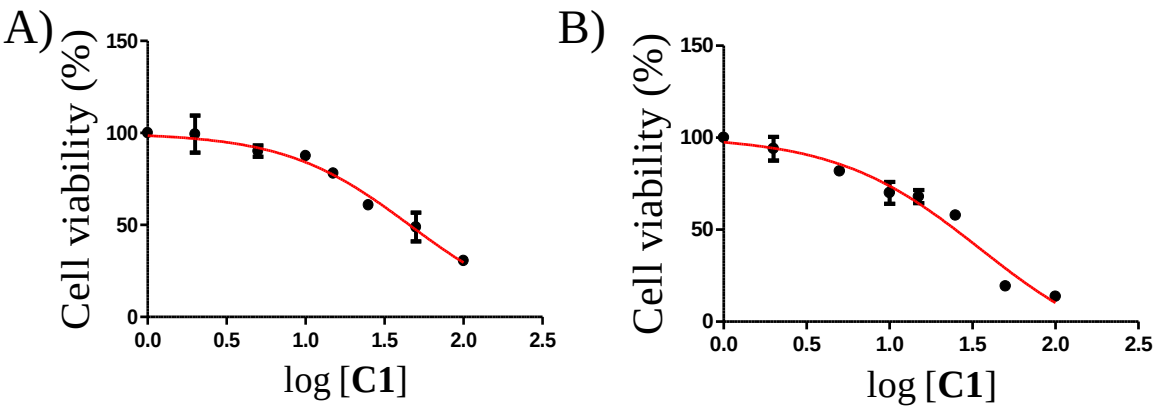

Fig. S11 Plots of cell viability (%) vs. log of concentration for **C1** A) MCF-7 and B) A549 cell lines after incubation for 48 h determine from MTT assays under normoxic condition. The plots provided are for one independent experiment out of the three independent experiments performed with each concentration.

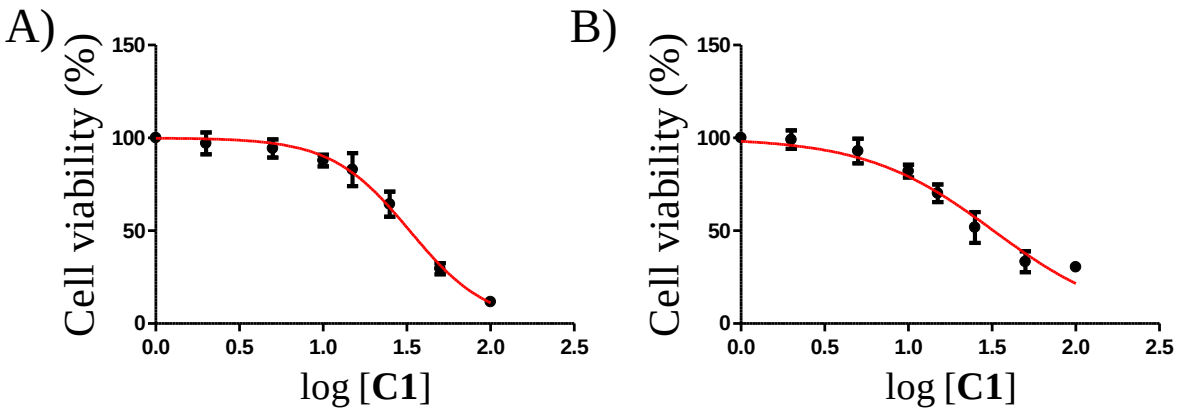

Fig. S12 Plots of cell viability (%) vs. log of concentration for **C1** A) MCF-7 and B) A549 cell lines after incubation for 48 h determine from MTT assays under hypoxic condition. The plots provided are for one independent experiment out of the three independent experiments performed with each concentration.

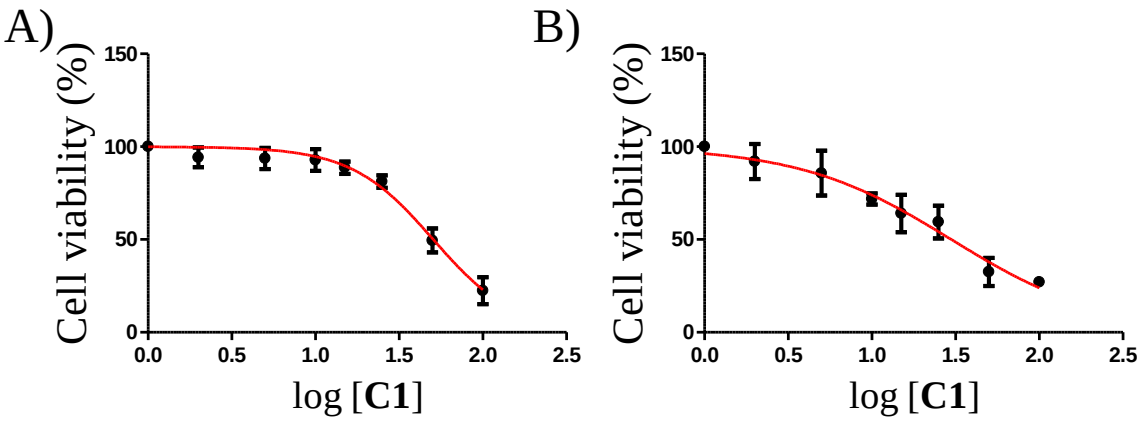

Fig. S13 Plots of cell viability (%) vs. log of concentration for **C1** A) MCF-7 and B) A549 cell lines after incubation for 48 h determine from MTT assays under hypoxic condition in presence of 1 mM L-glutathione. The plots provided are for one independent experiment out of the three independent experiments performed with each concentration.

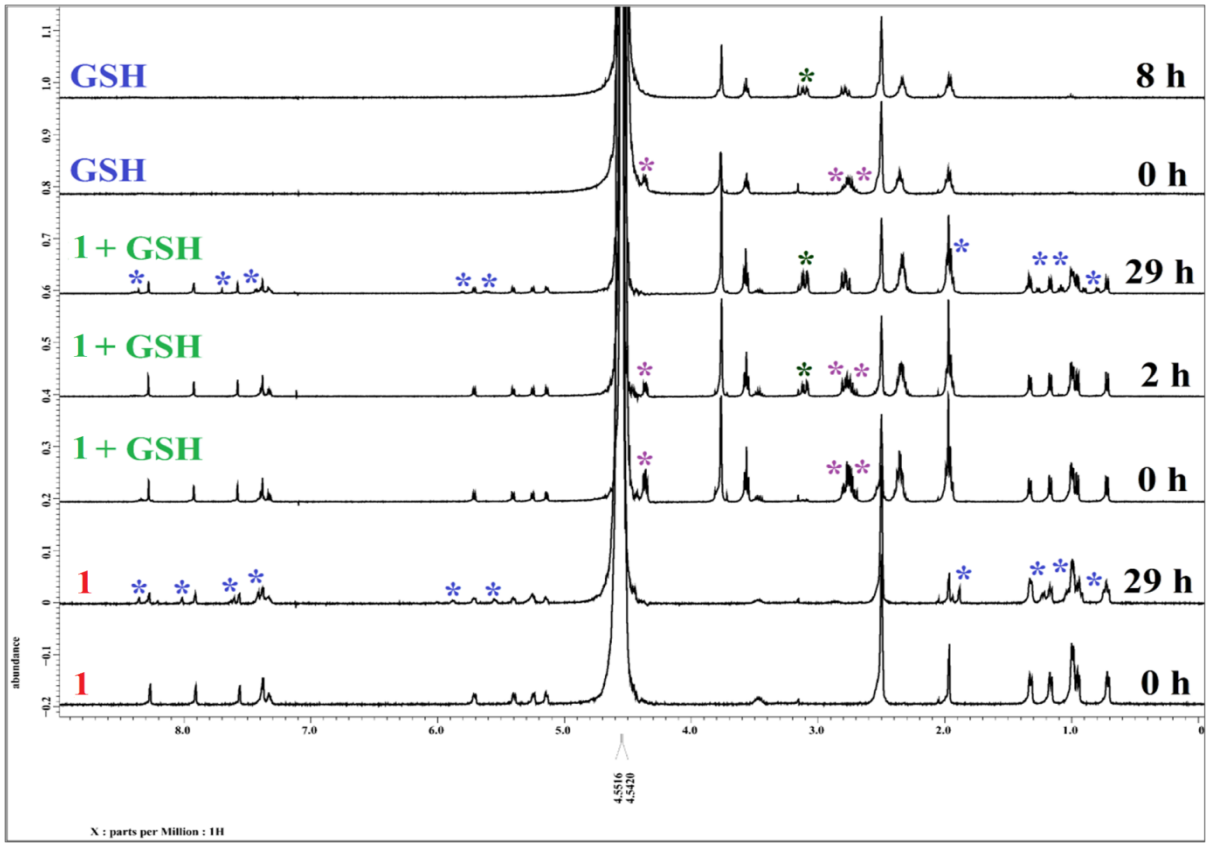

Fig. S14 Stack plot of ^{1}H NMR spectra of reduced L-glutathione at 0 h and 8 h (first two above), complex **1** at 0 h and 29 h (last two below), complex **1** and reduced L-glutathione (middle three) in 30% DMSO-d_6/D_2O mixture, recorded at different interval of time at 25°C. t = 0 h, stands for the spectra recorded immediately after dissolving reduced L-glutathione or complex **1**. *stands for hydrolysis product, *stands for GSH auto oxidation product.

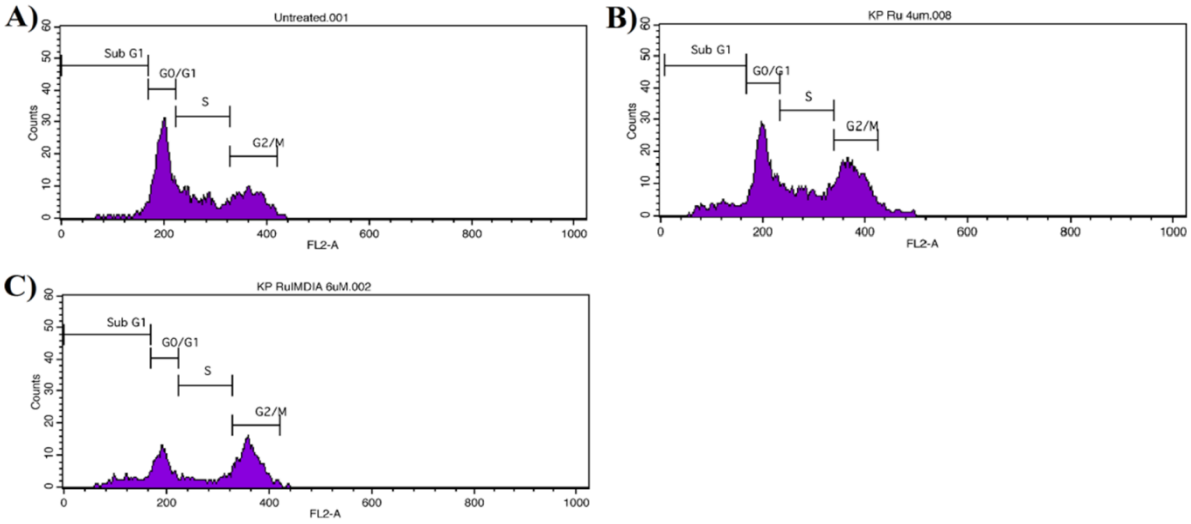

Fig. S15 Cell cycle analysis of MCF-7 treated with **1** for 24h. (A) DMSO control, (B) 4μM and (C) 6μM of **1** treated cells. The figure represents one independent experiment.

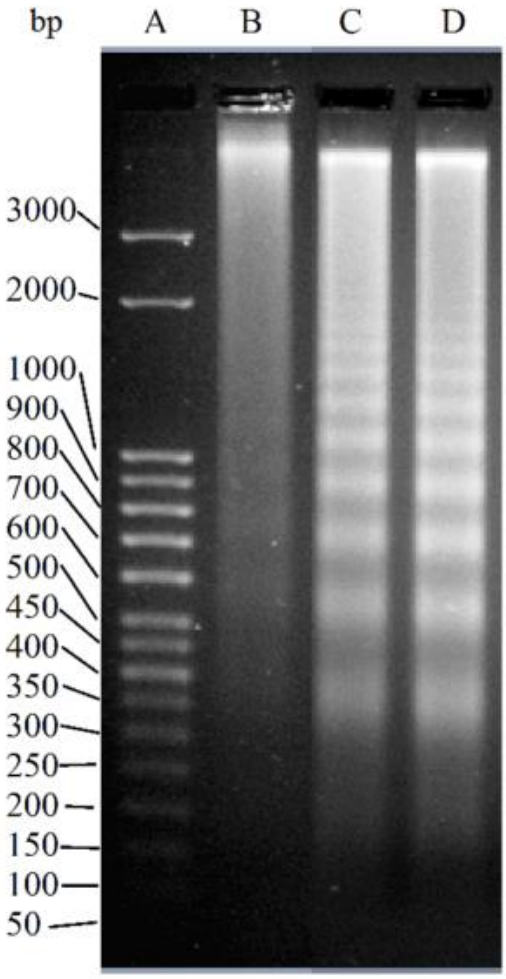

Fig. S16 Agarose gel image of DNA ladder formation due to apoptosis using MCF-7 cell line. (A) 50 bp step ladder, (B) DMSO control (C) **1** (6μM) (D) **1** (8μM) treated for 24 h.

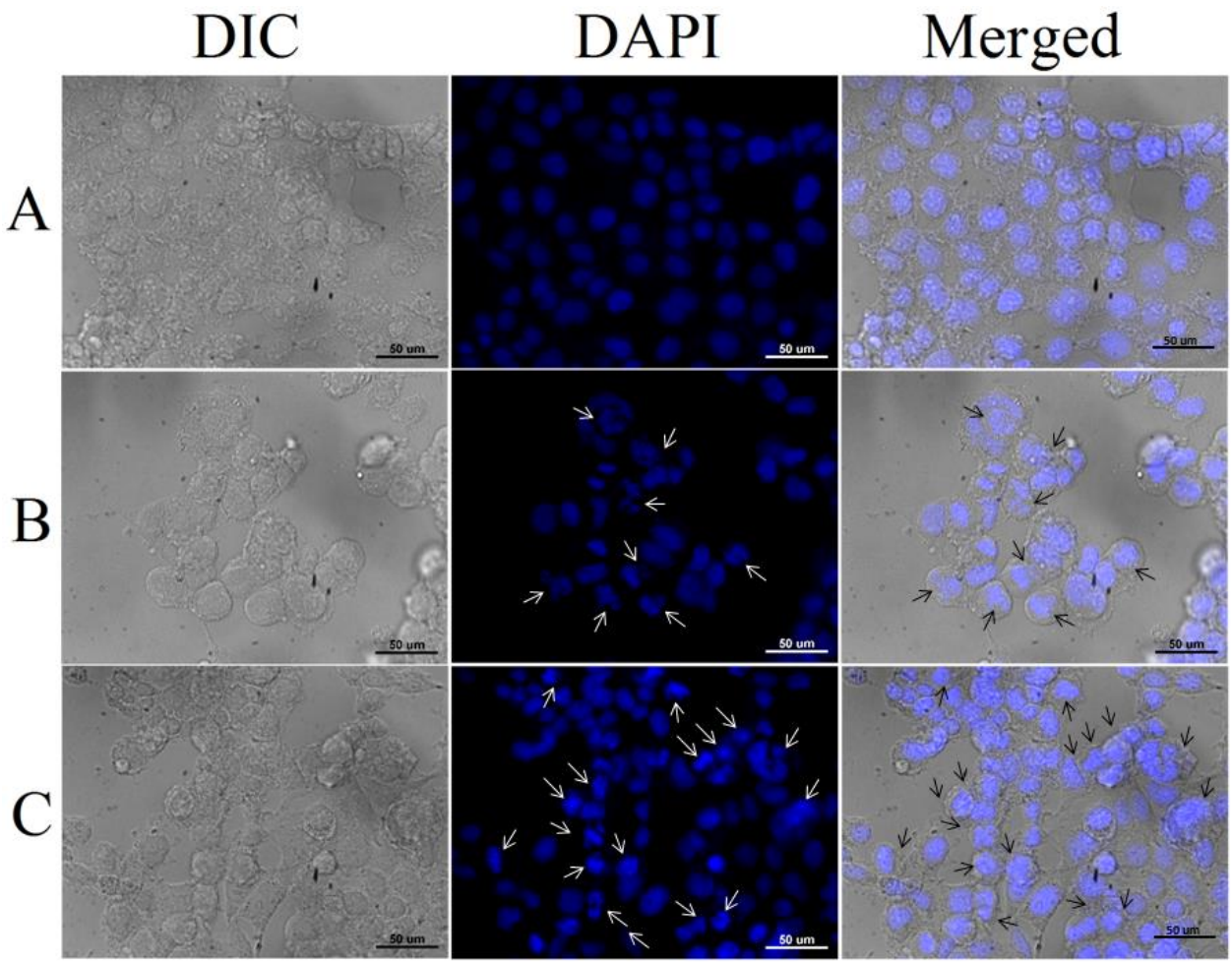

Fig. S17 Fluorescence microscopic images of MCF-7 after 24 h incubation with **1** (DAPI stained). The nuclear morphological changes in cells are indicated by arrows upon the treatment of **1**. (A) DMSO treated (< 0.2%); (B) **1** (6 μM) and (C) **1** (8 μM)

References.

1. D. D. Perrin and W. L. F. Armarego, *Purification of Laboratory Chemicals. 3rd Ed*, 1988.
2. M. A. Bennett, T. N. Huang, T. W. Matheson, A. K. Smith, S. Ittel and W. Nickerson, in *Inorganic Syntheses*, John Wiley & Sons, Inc., 2007, pp. 74-78.
3. *Application: WO*
   WO Pat., 1998-US3592
   9840420, 1998.
4. R. E. Morris, R. E. Aird, P. d. S. Murdoch, H. Chen, J. Cummings, N. D. Hughes, S. Parsons, A. Parkin, G. Boyd, D. I. Jodrell and P. J. Sadler, *J. Med. Chem.*, 2001, **44**, 3616-3621.
5. G. M. Sheldrick, *Z. Kristallogr.*, 2002, **217**, 644-650.
6. G. M. Sheldrick, *Int. Union Crystallogr., Crystallogr. Symp.*, 1991, **5**, 145-157.
7. C. Zhang, Y. Wang and F. Wang, *Bull. Korean Chem. Soc.*, 2007, **28**, 1183-1186.
8. J. Sangster and A. D. Pelton, *J. Phys. Chem. Ref. Data*, 1987, **16**, 509-561.
9. J. Marmur, *J. Mol. Biol.*, 1961, **3**, 208-218.
10. M. E. Reichmann, C. A. Rice, C. A. Thomas and P. Doty, *J. Am. Chem. Soc.*, 1954, **76**, 3047-3053.
11. K. Sengupta Tapas, M. Leclerc Gilles, T. Hsieh-Kinser Ting, J. Leclerc Guy, I. Singh and C. Barredo Julio, *Mol Cancer*, 2007, **6**, 46.
12. S. J. Dougan, A. Habtemariam, S. E. McHale, S. Parsons and P. J. Sadler, *Proc. Natl. Acad. Sci. U. S. A.*, 2008, **105**, 11628-11633.
13. A. K. Renfrew, A. D. Phillips, A. E. Egger, C. G. Hartinger, S. S. Bosquain, A. A. Nazarov, B. K. Keppler, L. Gonsalvi, M. Peruzzini and P. J. Dyson, *Organometallics*, 2009, **28**, 1165-1172.
14. F. Barragan, D. Carrion-Salip, I. Gomez-Pinto, A. Gonzalez-Canto, P. J. Sadler, R. de Llorens, V. Moreno, C. Gonzalez, A. Massaguer and V. Marchan, *Bioconjugate Chem.*, 2012, **23**, 1838-1855.
15. A. Kurzwernhart, W. Kandioller, E. A. Enyedy, M. Novak, M. A. Jakupec, B. K. Keppler and C. G. Hartinger, *Dalton Trans.*, 2013, **42**, 6193-6202.
16. K. J. Kilpin, S. Crot, T. Riedel, J. A. Kitchen and P. J. Dyson, *Dalton Trans.*, 2014, **43**, 1443-1448.
17. A. Kurzwernhart, W. Kandioller, C. Bartel, S. Baechler, R. Trondl, G. Muehlgassner, M. A. Jakupec, V. B. Arion, D. Marko, B. K. Keppler and C. G. Hartinger, *Chem. Commun.*, 2012, **48**, 4839-4841.
18. A. Kurzwernhart, W. Kandioller, S. Baechler, C. Bartel, S. Martic, M. Buczkowska, G. Muehlgassner, M. A. Jakupec, H.-B. Kraatz, P. J. Bednarski, V. B. Arion, D. Marko, B. K. Keppler and C. G. Hartinger, *J. Med. Chem.*, 2012, **55**, 10512-10522.
19. J. Kljun, A. K. Bytzek, W. Kandioller, C. Bartel, M. A. Jakupec, C. G. Hartinger, B. K. Keppler and I. Turel, *Organometallics*, 2011, **30**, 2506-2512.
20. S. J. Dougan, M. Melchart, A. Habtemariam, S. Parsons and P. J. Sadler, *Inorg. Chem.*, 2006, **45**, 10882-10894.
21. S. Betanzos-Lara, O. Novakova, R. J. Deeth, A. M. Pizarro, G. J. Clarkson, B. Liskova, V. Brabec, P. J. Sadler and A. Habtemariam, *JBIC, J. Biol. Inorg. Chem.*, 2012, **17**, 1033-1051.
22. I. Berger, M. Hanif, A. A. Nazarov, C. G. Hartinger, R. O. John, M. L. Kuznetsov, M. Groessl, F. Schmitt, O. Zava, F. Biba, V. B. Arion, M. Galanski, M. A. Jakupec, L. Juillerat-Jeanneret, P. J. Dyson and B. K. Keppler, *Chem. - Eur. J.*, 2008, **14**, 9046-9057.
23. K. J. Kilpin, S. M. Cammack, C. M. Clavel and P. J. Dyson, *Dalton Trans.*, 2013, **42**, 2008-2014.
24. A. K. Renfrew, A. D. Phillips, E. Tapavicza, R. Scopelliti, U. Rothlisberger and P. J. Dyson, *Organometallics*, 2009, **28**, 5061-5071.
25. A. D. Phillips, O. Zava, R. Scopelitti, A. A. Nazarov and P. J. Dyson, *Organometallics*, 2010, **29**, 417-427.
26. L. He, S.-Y. Liao, C.-P. Tan, R.-R. Ye, Y.-W. Xu, M. Zhao, L.-N. Ji and Z.-W. Mao, *Chem. - Eur. J.*, 2013, **19**, 12152-12160.
27. F. Wang, A. Habtemariam, E. P. L. van der Geer, R. Fernandez, M. Melchart, R. J. Deeth, R. Aird, S. Guichard, F. P. A. Fabbiani, P. Lozano-Casal, I. D. H. Oswald, D. I. Jodrell, S. Parsons and P. J. Sadler, *Proc. Natl. Acad. Sci. U. S. A.*, 2005, **102**, 18269-18274.

28. R. E. Aird, J. Cummings, A. A. Ritchie, M. Muir, R. E. Morris, H. Chen, P. J. Sadler and D. I. Jodrell, *Br. J. Cancer*, 2002, **86**, 1652-1657.
29. S. H. van Rijt, A. J. Hebden, T. Amaresekera, R. J. Deeth, G. J. Clarkson, S. Parsons, P. C. McGowan and P. J. Sadler, *J. Med. Chem.*, 2009, **52**, 7753-7764.
30. N. Busto, J. Valladolid, C. Aliende, F. A. Jalón, B. R. Manzano, A. M. Rodríguez, J. F. Gaspar, C. Martins, T. Biver, G. Espino, J. M. Leal and B. García, *Chem. Asian J.,* 2012, **7**, 788-801.
31. N. Busto, J. Valladolid, M. Martinez-Alonso, H. J. Lozano, F. A. Jalon, B. R. Manzano, A. M. Rodriguez, M. C. Carrion, T. Biver, J. M. Leal, G. Espino and B. Garcia, *Inorg. Chem.*, 2013, **52**, 9962-9974.
32. T. Bugarcic, A. Habtemariam, J. Stepankova, P. Heringova, J. Kasparkova, R. J. Deeth, R. D. L. Johnstone, A. Prescimone, A. Parkin, S. Parsons, V. Brabec and P. J. Sadler, *Inorg. Chem.*, 2008, **47**, 11470-11486.
33. A. Habtemariam, M. Melchart, R. Fernandez, S. Parsons, I. D. H. Oswald, A. Parkin, F. P. A. Fabbiani, J. E. Davidson, A. Dawson, R. E. Aird, D. I. Jodrell and P. J. Sadler, *J. Med. Chem.*, 2006, **49**, 6858-6868.
34. T. Bugarcic, A. Habtemariam, R. J. Deeth, F. P. A. Fabbiani, S. Parsons and P. J. Sadler, *Inorg. Chem.*, 2009, **48**, 9444-9453.
35. S. Betanzos-Lara, A. Habtemariam, G. J. Clarkson and P. J. Sadler, *Eur. J. Inorg. Chem.*, 2011, **2011**, 3257-3264.
36. W. Kandioller, C. G. Hartinger, A. A. Nazarov, M. L. Kuznetsov, R. O. John, C. Bartel, M. A. Jakupec, V. B. Arion and B. K. Keppler, *Organometallics*, 2009, **28**, 4249-4251.